

Aliphatic poly(propylene dicarboxylate)s: Effect of chain length on thermal properties and crystallization kinetics

M. Soccio^a, N. Lotti^{a,*}, L. Finelli^a, M. Gazzano^b, A. Munari^a

^a Dipartimento di Chimica Applicata e Scienza dei Materiali, Università di Bologna, Viale Risorgimento 2, 40136 Bologna, Italy

^b Istituto per la Sintesi Organica e la Fotoreattività, CNR, Via Selmi 2, 40126 Bologna, Italy

Received 13 February 2007; received in revised form 30 March 2007; accepted 4 April 2007

Available online 10 April 2007

Abstract

Polyesters based on 1,3-propanediol glycol and aliphatic dicarboxylic acids with different chain length were synthesized by melt polycondensation, obtaining samples characterized by high and comparable M_n . The polymers were subjected to molecular and thermal characterization. All polymers showed a good thermal stability, even though depending on the chain length. At room temperature all the polymers appeared as semicrystalline materials; the effect of the chain length was a lowering in the T_g value, an odd–even fluctuation for T_m and an increase of the crystallization rate. A comparison of the X-ray data revealed that the polymers with odd carbon number per repeat unit, show similar patterns, different from those of samples with even carbon atoms number. Multiple endotherms were evidenced in melt isothermally crystallized samples, due to melting and recrystallization processes. By applying the Hoffman–Weeks' method, the T_m^0 of the samples was derived. Lastly, the presence of an interphase was not evidenced.

© 2007 Elsevier Ltd. All rights reserved.

Keywords: Aliphatic polyesters; Melt polycondensation; Thermal properties

1. Introduction

The past two decades have witnessed a growing public and scientific concern regarding the use of biodegradable plastic material as a solution for the problem of plastic waste. Several biodegradable polymers have been successfully developed over the past years to meet the specific demands, e.g., in agriculture, packaging and pharmaceutical industries [1,2]. The best understood and most extensively studied plastics with regard to biodegradation are poly(hydroxyalkanoates) (PHA), which are polymers naturally produced by bacteria [3,4]. However, for practical applications biodegradable aliphatic synthetic polyesters such as poly(ϵ -caprolactone) (PCL), poly(ethylene succinate-*co*-butylene succinate) (trade name “Bionolle”) and polylactide (PLA) have predominantly been

used up to now [5]. Due to the limited properties of some aliphatic polyesters, new biodegradable aliphatic–aromatic copolyesters have been also developed and recently introduced into the market, e.g., under the trade name Ecoflex (BASF AG, Germany) or Eastar Bio (Eastman Chemicals, U.S.A.) [6,7]. These polyesters show a wide variety in their physical and mechanical properties being in some cases directly comparable with that of many traditional and nonbiodegradable polymers, especially low-density polyethylene (LDPE) and polypropylene (PP). Polyesters based on 1,3-propanediol glycol (1,3-PD) have attracted increasing interest only in the last few years. This was a consequence of the fact that in the past 1,3-PD was not available in the market at low cost and in sufficient purity. However, recently more attractive processes have been developed for its production, such as selective hydration of acrolein followed by catalytic hydrogenation of the intermediate 3-hydroxypropionaldehyde [8,9], or hydroformylation of ethylene oxide [10]. Currently, Du Pont and Shell Chemical companies have developed 1,3-propanediol

* Corresponding author. Tel.: +39 051 2093202; fax: +39 051 2093220.

E-mail address: nadia.lotti@mail.ing.unibo.it (N. Lotti).

commercial product with low cost and high quality by using biotechnological methods: in particular, Du Pont's fiber-grade, or apparel-grade 1,3-PD has successfully been prepared by a fermentation process of corn sugar, a renewable resource [11]; Shell has produced 1,3-PD via an enzymatic fermentation of glycerine [12]. 1,3-PD is really considered to be one of the bulk chemicals that will be produced in large scale in the next few years and consequently, its polycondensates are now arousing an increasing interest both from the academic and industrial point of view.

It is well known that crystallization is a phase transition that plays an important role in determining the morphology of a polymer for a wide range of technological processes, in which commodities are formed from synthetic plastics. Moreover, because the crystal structure and morphology (the crystal habit and organization of crystals into aggregates of a higher order) are responsible for many properties of the final products, the knowledge of the crystallization mechanisms is crucial for designing materials with the required properties.

Furthermore, in recent years, the study of the rigid-amorphous phase present in some polymers has aroused a growing interest [13–17]. Generally, the highly ordered structure of most semicrystalline polymers cannot be simply described by means of a two-phase model, consisting of crystalline and amorphous phases. As a consequence, a third phase, the so-called 'rigid-amorphous phase' (RAP) or 'interphase' between crystalline and amorphous layers has been taken into consideration in the structure. RAP is defined as that portion of noncrystalline material that does not mobilize at T_g and, therefore, does not contribute to the observed Δc_p value. Its importance derives from the fact that the interphase is often correlated with the presence of a very disperse crystalline phase, influencing consequently the final mechanical properties of the polymer.

In this view, herein the results of a detailed investigation of the thermal properties and crystallization kinetics of some new aliphatic biodegradable polyesters based on 1,3-propanediol and aliphatic dicarboxylic acid with different chain length, synthesized in our laboratories by melt polycondensation procedure, are reported. Aim of the research is to investigate the effect of chain length on the thermal properties and crystallization kinetics of such polymers.

2. Experimental

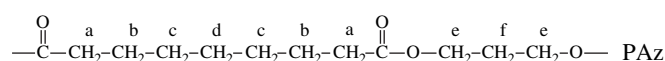
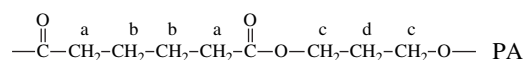
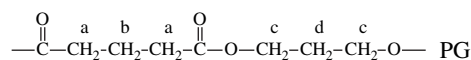
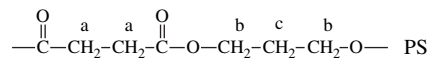
2.1. Products

Dimethylsuccinate (DMS), dimethylglutarate (DMG), dimethyladipate (DMA), dimethylazelate (DMAz), 1,3-propanediol (1,3-PD) and titanium tetrabutoxide ($\text{Ti}(\text{OBU})_4$) (Aldrich) are reagent grade products; all the reagents were used as supplied, except $\text{Ti}(\text{OBU})_4$ that was distilled before use.

2.2. Synthesis of polymer samples

Poly(propylene succinate) (PPS), poly(propylene glutarate) (PPG), poly(propylene adipate) (PPA) and poly(propylene

azelate) (PPAz) were synthesized in bulk starting from the appropriate dimethylcarboxylate and PD glycol in a molar ratio 1:2, employing $\text{Ti}(\text{OBU})_4$ as catalyst (about 0.2 g of $\text{Ti}(\text{OBU})_4$ /kg of polymer). The syntheses were carried out in a 200 mL stirred glass reactor, with a thermostatted silicon oil bath; temperature and torque were continuously recorded during the polymerization. The polymers were prepared according to the usual two-stage polymerization procedure. In the first stage, under pure nitrogen flow, the temperature was raised to 180 °C and maintained there for until more than 90% of the theoretical amount of methanol was distilled off (about 2 h). In the second stage the pressure was reduced (about 0.1 mbar), in order to facilitate the removal of the glycol in excess and the temperature was kept at 210 °C until a torque constant value was measured. The polymers obtained, because of the use of $\text{Ti}(\text{OBU})_4$ as catalyst and the high temperature, which favour redistribution reactions, are statistical. The monomeric units of poly(propylene dicarboxylate)s investigated are the following:



2.3. ^1H NMR spectroscopy

The chain structure of the polymers was determined by means of ^1H NMR spectroscopy. Polymer samples were dissolved (15 mg/mL) in chloroform-*d* solvent with 0.03% (v/v) tetramethylsilane added as an internal standard. The measurements were carried out at room temperature, employing a Varian INOVA 400 MHz instrument.

2.4. Gel-permeation chromatography

Molecular weight data were obtained by gel-permeation chromatography at 30 °C using a 1100 Hewlett Packard system equipped with PL gel 5 μ MiniMIX-C column (250/4.6 length/i.d., in mm). A refractive index was employed as detector. In all cases, chloroform was used as eluent with a 0.3 mL/min flow, and sample concentrations of about 2 mg/mL were applied. A molecular weight calibration curve was obtained with several polystyrene standards in the range of molecular weight 2000–100,000.

2.5. Wide-angle X-ray measurements

X-ray diffraction measurements were carried out at room temperature with a Bragg/Brentano diffractometer system (Panalytical X'Pert), equipped with a real time multiple strip

X'Celerator detector. Cu anode was used as X-ray source ($\lambda = 0.15418$ nm); the data were collected in the 2θ range from 5 to 60° in 3 min. A 0.25° divergence and 0.25° anti-scatter slits were used.

2.6. Thermal analysis

2.6.1. TG measurements

Thermogravimetric analysis was carried out both in air and under nitrogen atmosphere using a Perkin–Elmer TGA7 apparatus (gas flow: 40 mL/min) at 10 °C/min heating rate up to 900 °C. The procedure suggested by the supplier was followed for the temperature calibration of equipment. This method is based on the change of the magnetic properties of two metal samples (nickel and perkalloy) at their Curie points (354.0 and 596.0 °C, respectively). The T_{onset} at which the weight loss starts was taken as temperature of initial decomposition (T_{id}).

2.6.2. DSC measurements

Calorimetric measurements were carried out by means of a Perkin–Elmer DSC7 instrument equipped with a liquid sub ambient accessory and calibrated with high purity standards (indium and cyclohexane). With the aim of measuring the glass transition and the melting temperatures of the polymers under investigation, the external block temperature control was set at -120 °C and weighed samples of ca. 10 mg were encapsulated in aluminum pans and heated to about 40 °C above fusion temperature at a rate of 20 °C/min (first scan), held there for 3 min, and then rapidly quenched (about 100 °C/min) to -80 °C. Finally, they were reheated from -80 °C to a temperature well above the fusion temperature of the sample at a heating rate of 20 °C/min (second scan). The glass transition temperature T_g was taken as the midpoint of the heat capacity increment Δc_p associated with the glass-to-rubber transition. The melting temperature (T_m) was determined as the peak value of the endothermic phenomenon in the DSC curve. The specific heat increment Δc_p , associated with the glass transition of the amorphous phase, was calculated from the vertical distance between the two extrapolated baselines at the glass transition temperature. The heat of fusion (ΔH_m) of the crystal phase was calculated from the area of the DSC endotherm.

The study of the crystallization kinetics of the samples under isothermal conditions, was performed by means of DSC measurements carried out under a nitrogen atmosphere, by using a fresh specimen (ca. 5 mg) for each run, employing the following standard procedure: the samples were heated to about 40 °C above fusion temperature, held there for 3 min, then quenched to the crystallization temperature T_c . The heat flow evolving during the isothermal crystallization was recorded as a function of time and the completion of the crystallization process was detected by the levelling of the DSC trace. For a better definition of the starting time, a blank run was also performed with the same sample for each isothermal scan, at a temperature above the melting point where no phase change occurred [18]. The blank run was subtracted from the

isothermal crystallization scan and the start of the process was taken as the intersection of the extrapolated baseline and the resulting exothermal curve. The isothermally crystallized samples were then heated directly from T_c to melting point at 10 °C/min.

To gain information about the presence of a rigid-amorphous phase in the samples under investigations, specimens characterized by different crystal/amorphous phase ratios were investigated. These samples were obtained by partial melting in DSC by heating to various temperatures in the melting range, quickly cooled inside the instrument below the glass transition temperature and reheated at 20 °C/min.

Repeated measurements on each sample showed excellent reproducibility.

3. Results and discussion

3.1. Molecular characterization

At room temperature the as-synthesized polyesters are transparent and light yellow coloured with the exception of PPAz which is opaque. Their solubility was checked in various solvents: all the samples showed a good solubility at room temperature in the most common organic solvents, i.e. chloroform, tetrachloroethane, methylene chloride, etc. Before molecular and thermal characterization, all the polymers were carefully purified by dissolution in chloroform and precipitation in cold methanol. Finally, the samples were kept in a vacuum oven at room temperature several days in order to remove the residual solvent. The purified polymers appear as semi-crystalline white solids and their characteristics are collected in Table 1.

First of all, it can be noted that all the polymers are characterized by molecular weights, significantly higher than those of analogous aliphatic polyesters synthesized by others previously [19]. This can be considered as a proof that appropriate polymerization conditions and a good polymerization control were obtained.

In order to have an understanding into the chemical structure, the ^1H NMR investigation on the samples was performed. In all cases, the spectra were found to be consistent with the expected structure, indicating that no side reaction occurs during the syntheses. The chemical shift assignments (δ , ppm) are the following: PPS: δ 1.95 (quin, 2H^c), δ 2.60 (s, 4H^a), δ 4.16 (t, 4H^b); PPG: δ 1.91 (quin, 2H^b), δ 1.94 (quin, 2H^d), δ 2.35 (t, 4H^a), δ 4.12 (t, 4H^c); PPA: δ 1.64 (quin, 4H^b), δ 1.92 (quin, 2H^d), δ 2.26 (quin, 4H^a), δ 4.15 (t, 4H^c); PPAz: δ 1.32 (m, 6H^{cd}), δ 1.60 (m, 4H^b), δ 1.96 (quin, 2H^f), δ 2.29 (m, 4H^a), δ 4.14 (t, 4H^e) (see the chemical structures reported in Section 2).

3.2. Thermal properties

The polyesters were afterwards examined by thermogravimetric analysis and differential scanning calorimetry. The investigation on the thermal stability was carried out both in

Table 1
Molecular and thermal characterization data

Polymer	M_n	T_{id} (°C)	First scan				Second scan			
			T_g (°C)	Δc_p (J/g °C)	T_m (°C)	ΔH_m (J/g)	T_g (°C)	Δc_p (J/g °C)	T_m (°C)	ΔH_m (J/g)
PPS	36,400	361	-27	0.34	44	40	-29	0.66	—	—
PPG	43,500	374	-47	0.21	54	59	-49	0.62	—	—
PPA	31,200	340	-52	0.37	40	49	-54	0.61	—	—
PPAz	36,000	380	-52	0.07	57	78	-58	0.23	49	56

air and under nitrogen atmosphere. Fig. 1 shows the thermogravimetric curves of the samples under nitrogen atmosphere.

It can be seen that in all cases the weight loss takes place in one-step and the thermogravimetric curves are characterized by the same char residue (about 5%). Moreover, as evidenced by the temperature of initial decomposition (T_{id}) reported in Table 1, all the samples are characterized by a relatively high thermal stability, the T_{id} values ranging from 340 to 380 °C. Anyway, significant effect of the chemical structure of the polymer on its thermal stability can be observed. As is well known, at lower temperatures, linear aliphatic polyesters undergo depolymerisation to linear and cyclic esters or lactones, a reaction commonly employed in the syntheses of many of such substances; at higher temperatures, a further decomposition ensues, typically with the formation of vinyl and carboxyl groups by ester scission and by cyclic elimination mechanism; a four-centre cleavage to ketene groups has also been proposed [20]. As reported in the literature [21], the main thermal degradation pathway of polyesters is highly dependent on the chain length of the diol subunit, whereas the influence of the dicarboxylic acid one is less important [21]. In our case, the different thermal stability of the polyesters synthesized cannot be explained on these bases as the diol subunit is the same for all the polymers under investigation. Therefore, the observed behaviours have to be ascribed to different mechanisms in the decomposition of the dicarboxylic acid subunits. The simplest way to interpret our results is to consider that in many cases aliphatic polyesters can be

assimilated to polyethylene chains containing ester groups. In this view, it is well established that the introduction of ester linkages into the polyethylene chain reduces its thermal stability, the effect being proportional to their concentration [22]. Therefore, it is not surprising that PPAz appears to be the most thermally stable among the aliphatic polyesters under investigation and that PPG is characterized by a higher thermal stability with respect to PPS. An anomalous behaviour is shown by PPA, which turns out to be the least stable polymer. Recently, Schulten and Plage [21] studied several aliphatic polyesters by means of pyrolysis-field ionization mass spectroscopy in order to investigate the degradation mechanisms. In particular, the authors paid attention to PPS and PPA: as far as PPS is concerned, the main degradation products were propionaldehyde and cyclic succinic anhydride; in the case of PPA, three products have been recognized, i.e. butyrodiketene, cyclopentanone and a cyclic anhydride constituted by a stable seven-membered ring. It has to be emphasized that diketenes do not form from other dicarboxylic acid subunits and this result has been explained on the basis of the chain length. Moreover, the results obtained [21] showed that the adipic acid subunit is the only responsible for cyclopentanone formation, which undoubtedly represents a favourable five-membered ring [21]. In the case of PPS and PPG the much less favourable cyclopropanone and cyclobutanone formation can be hypothesized, respectively, and therefore the higher thermal stability of PPS and PPG with respect to PPA can be explained.

As regards calorimetric results, being the samples characterized by high M_n s, an influence of molecular weight on the glass transition and melting of the polymers synthesized can be excluded. It is well established that the melting behaviour of a polymer is affected by its previous thermal history and therefore, in order to provide the same heat treatment to all the samples investigated, prior to thermal analysis the specimens have been aged for a very long time (about six months) at room temperature in desiccators. The DSC traces of such samples are reported in Fig. 2 and the data obtained in Table 1. Moreover, as is well known, a partially crystalline material usually exhibits a different glass transition behaviour than the completely amorphous analogous. In fact, although some conflicting results are reported in the literature [23], crystallinity usually acts like cross-linking and raises T_g through its restrictive effect on the segmental motion of amorphous polymer chains. Therefore, in order to study the influence of the chemical structure on the glass transition of a polymer, the phenomenon should be examined in the total absence of crystallinity. In this view, all the samples under investigation were subjected

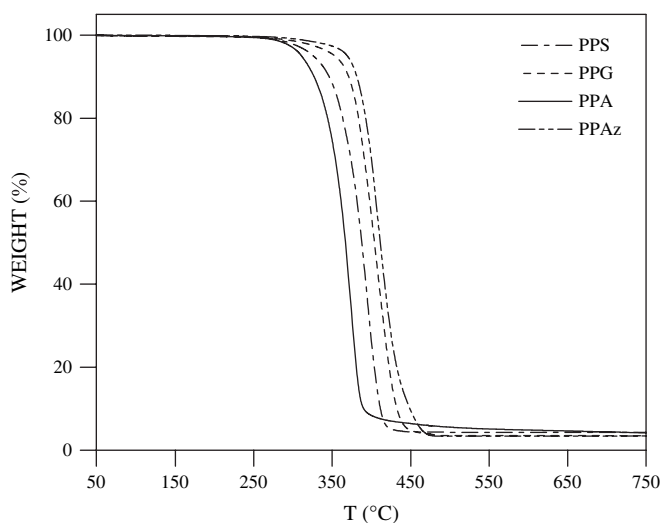


Fig. 1. Thermogravimetric curves under nitrogen atmosphere (10 °C/min).

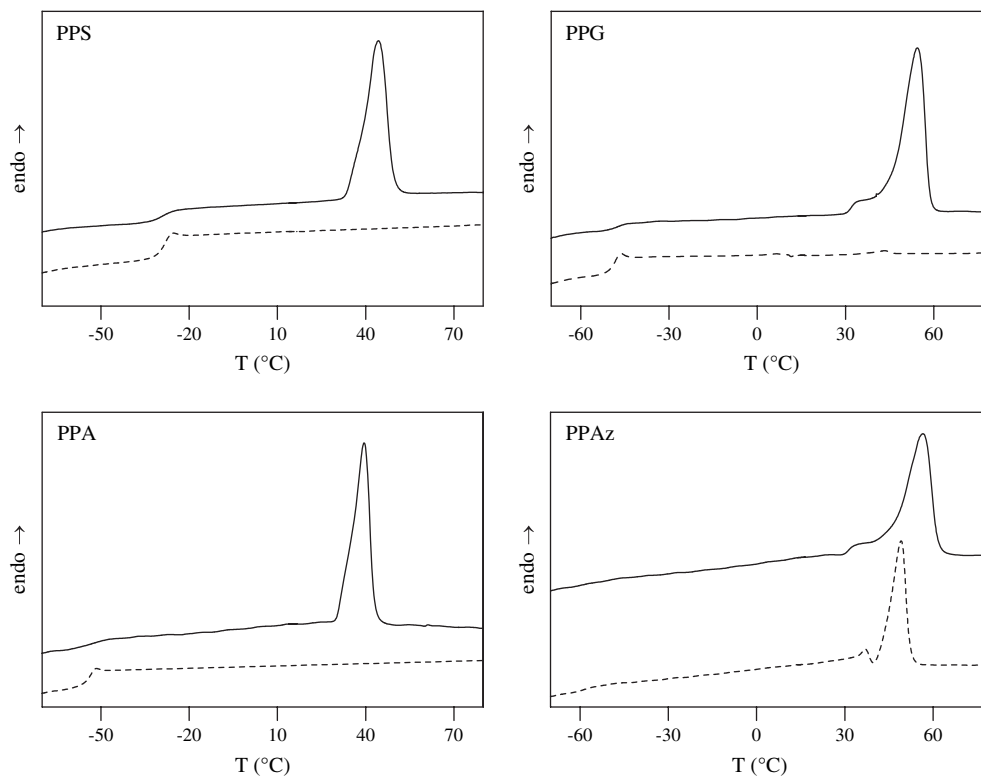


Fig. 2. First scan (full line); second scan after melt quenching (dashed line).

to rapid cooling (quenching) from the melt (see Section 2 for details). The DSC curves after melt quenching are also shown in Fig. 2 and the data collected in Table 1.

As far as the DSC traces of the room-stored samples are concerned (first scan), they are typical semicrystalline material, being characterized by the presence of a conspicuous melting endotherm. After melt quenching, the phase behaviour of the samples under investigation appears to be different: PPS, PPG and PPA are found to be completely amorphous, their DSC traces being characterized only by an endothermal baseline deviation associated with the glass transition phenomenon. On the contrary, PPaz is found to be partially crystalline, as proved by the presence in its calorimetric curve of a glass transition phenomenon followed by a conspicuous melting endotherm at higher temperature. This result demonstrates that this sample cannot be frozen into a completely amorphous state by quenching and therefore it is characterized by a high crystallization rate, much higher than those of the other polyesters under investigation. However, further comments on the crystallization rate can be more correctly made by analyzing the results of the isothermal crystallization experiments in DSC, reported in the following. The measured T_g and T_m values are reported in Fig. 3 as a function of the number of methylene group of the acid subunit.

First of all, it has to be emphasized that experimental glass transition temperature of PPaz value is expected to be little higher with respect to the one of the completely amorphous sample. As it can be seen, both T_g and T_m values are affected by the chemical characteristics of the macromolecules: the

melting temperature exhibits an odd–even effect, whereas the glass transition temperature decreases as the number of methylene group present in the monomeric unit is increased. As far as the T_m trend is concerned, it would be expected that polymers containing longer aliphatic chains are more flexible, thus crystallizing more readily and melting at lower temperature. The different behaviour observed for the poly-(alkylene dicarboxylate)s analyzed suggests that the chain

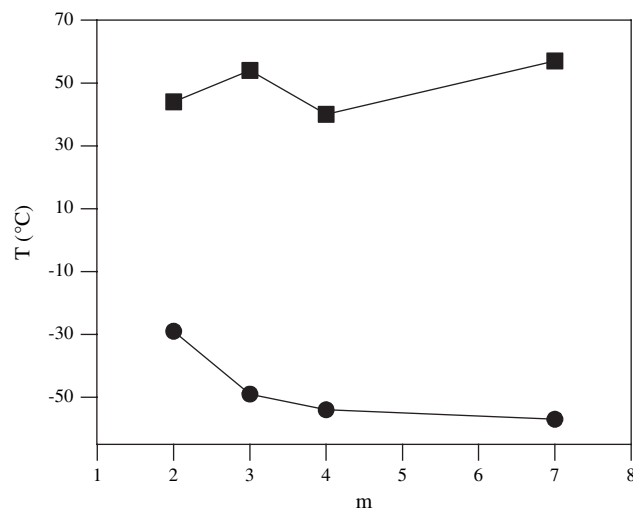


Fig. 3. Melting (■) and glass transition (●) temperatures of poly(propylene dicarboxylate)s as a function of the number of methylene group of the acid subunit (m).

flexibility is not the only parameter that has to be taken into consideration to explain the melting phenomenon. In particular, it can be noted that the polyesters with an even number of carbon atoms per repeat units, i.e. PPG and PPaz with 8 and 12 per repeat units, respectively, have higher melting points than PPS and PPA, which are characterized by an odd number of carbon atoms (7 and 9, respectively). Therefore, in addition to the chain flexibility, the characteristics of the crystal structure and the chain conformation have to be also considered to explain the observed trend. In order to investigate these results more deeply, further experiments by using X-ray diffractometry are currently being carried out. Comparing the melting temperatures of the two polyesters with an odd number of carbon atoms per repeat unit, i.e. PPS and PPA, one can see that T_m value decreases as the aliphatic chain length is increased, as expected on the basis of an increment of the chain flexibility. On the contrary, if we consider the melting temperatures of the two aliphatic polyesters with an even number of carbon atoms, i.e. PPG and PPaz, the trend found is opposite: T_m value increases as the aliphatic chain length is increased. The observed increment of the melting temperature with the increment of the methylene groups per repeat unit can be interpreted as a tendency of the polymer to adopt the crystalline conformation and to reach the melting temperature of poly(ethylene) (PE). The ester functionalities act as defects in the polyethylene backbone: T_m increases as the distance between two consecutive ester groups is increased, thus the number of defects decreases.

The T_g trend, i.e. the fact that the glass transition temperature steadily decreases as the number of $-(CH_2)-$ groups per repeat unit is increased, can be explained on the basis of an increment of chain flexibility: as a matter of fact, the higher is the number of methylene groups in the polymeric chain the lower the concentration of the stiffer ester groups (O–CO–). As a consequence, the polymeric chain is more flexible and thus the polymer has a lower T_g .

To check the structure of the crystalline phase in the samples under investigation and to correlate it to the chemical structure, X-ray diffractometry measurements were performed at room temperature. The diffraction curves for PPS, PPG, PPA and PPaz are reported in Fig. 4.

The only X-ray spectra reported in the literature is that of PPS [19]: the pattern obtained by us is very similar to the one published. As far as PPA is concerned, one can see that its XRD pattern is characterized by strong reflections at 19.0, 20.9, 22.2, and 24.3° ($d=0.466$, 0.425, 0.401, and 0.365 nm) and by weaker reflections at 8.20, 16.9, 26.9, and 29.4° ($d=1.07$, 5.24, 3.31, and 3.03 nm). Moreover, it can be noted that PPA X-ray diffraction profile is resembling to that of PPS: the X-ray profiles of the two aliphatic polyesters with an odd number of carbon atoms per repeat unit are indeed characterized by several peaks of comparable relative intensity even though shifted to lower angles (longer interplanar distances) in the case of PPA. Therefore, a possible isomorphous structure of the two polyesters can be hypothesized. As far as the two aliphatic polyesters characterized by an even number of carbon atoms per repeat unit (PPG and PPaz), it can be

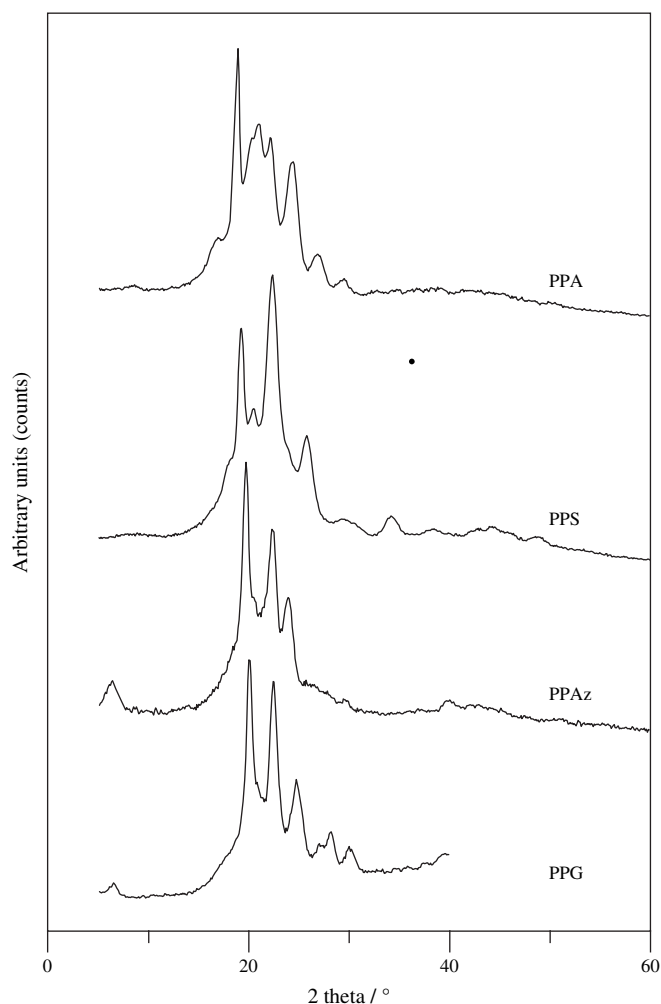


Fig. 4. Wide-angle X-ray diffraction profile of the poly(propylene dicarboxylate)s.

noted that the corresponding profiles are also very similar to each other: both X-ray spectra show indeed a low angle reflection ($2\theta = 6.4^\circ$) and three intense reflections between 20 and 25°. The PPaz reflections are slightly shifted at higher angles with respect to those of PPG. On the contrary, PPS and PPA X-ray spectra are appreciably different from those of PPG and PPaz. Taking into account that the kind of pattern is strictly correlated to the crystal structure, a different packing should be hypothesized for the even or odd number of carbon atoms-containing polyester. To our knowledge, no data on crystal structure were reported in the literature for PPG, PPA and PPaz with the exception of the old data concerning fibers [24]. Further investigations of the crystal structures are in progress.

3.3. Isothermally crystallized samples

3.3.1. Melting behaviour

Fig. 5 shows some typical calorimetric traces of PPS, PPG, PPA and PPaz isothermally crystallized at various temperatures (T_c) according to the thermal treatment described in Section 2.

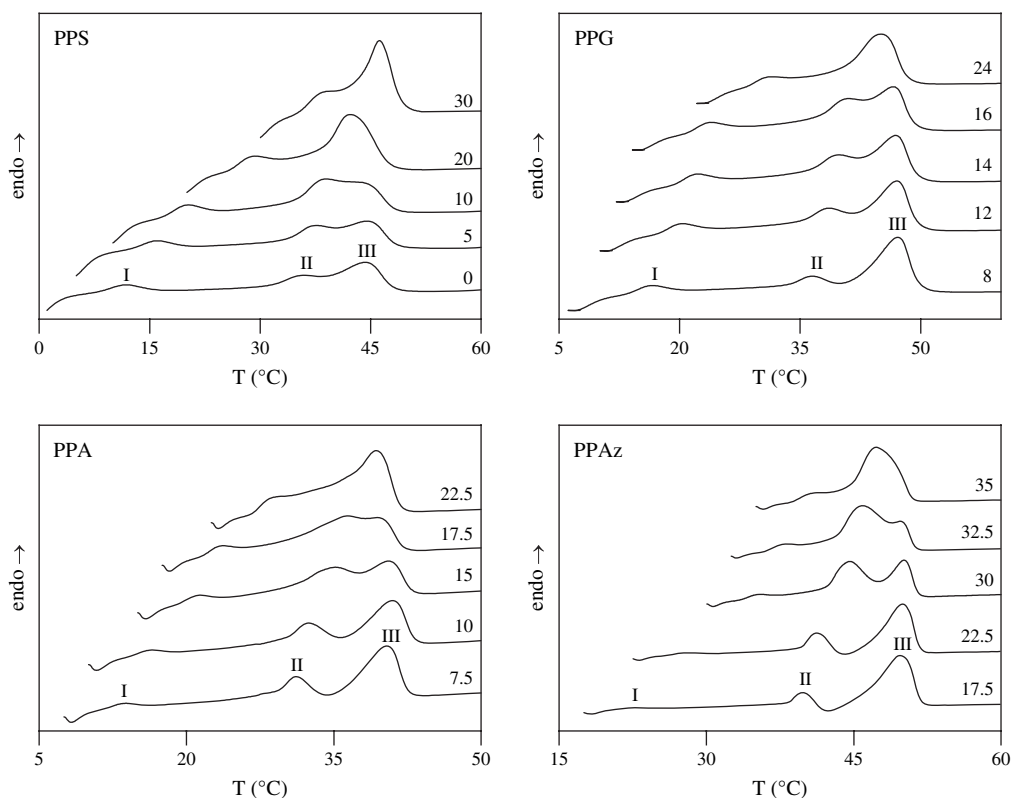


Fig. 5. DSC melting endotherms after isothermal crystallization at the indicated T_c 's (heating rate: 10 °C/min).

As can be seen, three endotherms appear in the thermograms on heating, whose peaks have been labeled with Roman numerals (I–III) in order of increasing temperature. A dependence of the position and intensity of the endotherms on temperature can be observed: in particular, endotherm I temperature is approximately 10 °C above T_c ; the position of melting peak II shifts to higher temperature and its magnitude increases with increasing the crystallization temperature. As regards endotherm III, its position remains unchanged, whereas the magnitude decreases with increasing T_c . At present, two main hypotheses have been proposed to account for the multiple melting behaviour: (i) melting and recrystallization processes occurring during the calorimetric run [25–27] and (ii) the existence of different crystal structures [28,29]. As regards the polyesters under investigation, the observed dependence of the multiple endotherms on crystallization temperature permits to hypothesize the origin of each peak. In particular, peak I can be considered as the typical “annealing peak” and can be associated with the melting of poorer crystals that grow at T_c between the larger crystals. Endotherm II can be ascribed to the fusion of crystals grown by normal primary crystallization during the isothermal period at T_c ; its dependence on the crystallization temperature, in terms of both peak position and area, suggests that thicker crystalline lamellae develop with increasing T_c . The high temperature melting peak (III) can be explained as the result of the melting of crystals of higher stability and perfection, grown during the heating run as a consequence of recrystallization or reorganization of crystals initially formed during isothermal crystallization.

In order to confirm the possibility of melting–recrystallization processes, the effect of the heating rate on the melting phenomenon was evaluated. As shown in Fig. 6, the magnitude of melting peak II increases as the heating rate is increased, contrarily to the high temperature melting peak III, the intensity of which regularly decreases with the heating rate.

The higher value of the heat of fusion of the melting peak II at the faster heating rate indicates that the crystals formed at T_c do not have enough time to melt and recrystallize, confirming therefore a mechanism based on melting and recrystallization of less perfect crystallites into thicker crystals melting at higher temperature. A further evidence that melting and recrystallization processes occur has been obtained performing wide-angle X-ray measurements on samples isothermally crystallized at different temperatures. In all cases, the WAXS patterns exhibit the same diffraction peaks, indicating that the samples are characterized by the same crystal structure at all the crystallization temperatures investigated.

Equilibrium melting temperature (T_m^0) is a parameter, which must first be determined in order to analyze crystal growth kinetics. Equilibrium melting temperature is defined as the melting temperature of lamellar crystals with an infinite thickness. However, it is impossible to obtain such lamellae in practice, because of kinetics factors. Thus, extrapolative methods are used to estimate T_m^0 . In this view, four general methods are used, including the Gibbs–Thomson and the Flory–Vrij approaches, the Hoffman–Weeks procedure [30], and the fitting of growth rate data at a sufficiently low supercooling with the classical theory of lamellar crystal

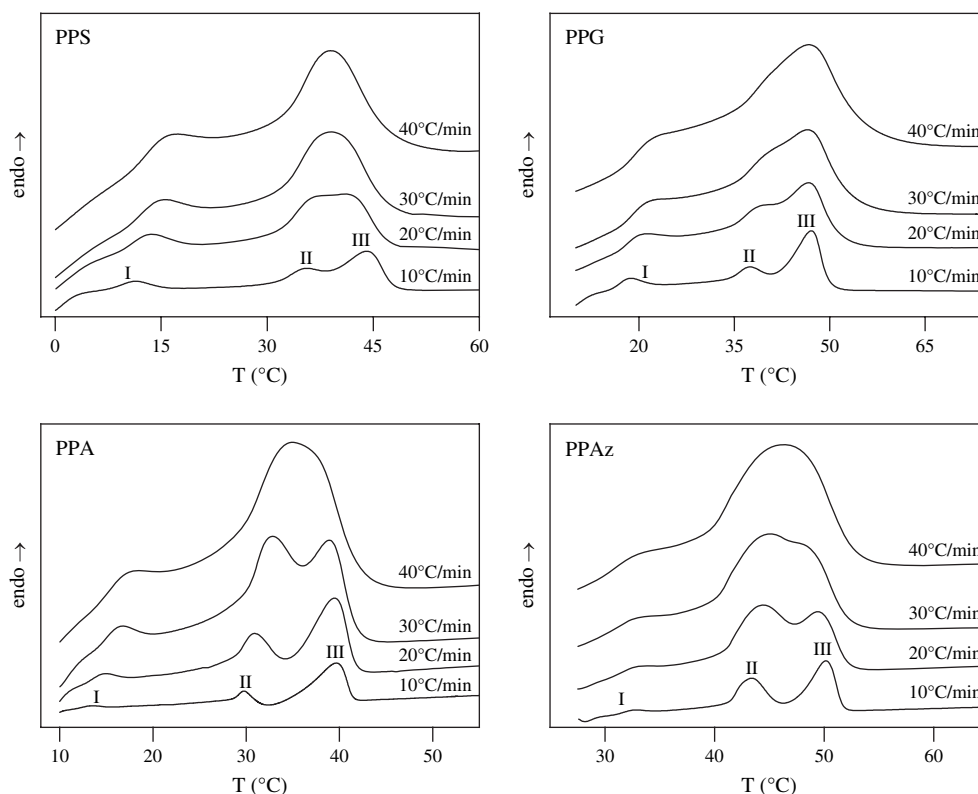


Fig. 6. DSC melting endotherms of PPS, PPG, PPA and PPAz scanned at the indicated heating rate after isothermal crystallization at 0, 10, 10 and 27.5 °C, respectively. The curves have not been corrected for changes in the thermal lag with the heating rate.

growth [31]. Among them, Hoffman–Weeks method is commonly used to estimate T_m^0 . However, there is criticism on the validity of this procedure. Recently, Marand and co-workers [31,32] discussed the validity of the assumption that represents the basic premise of the linear Hoffman–Weeks treatment: i.e. the thickening coefficient for lamellae, γ , is taken as independent of T_c and time. As demonstrated by some results [32,33] that appeared in the literature, the linear extrapolation, when carried out for lamellar crystals exhibiting a constant γ value, invariably underestimates the T_m^0 and leads to an overestimation of the γ value. In fact, the Hoffman–Week procedure does not account for a significant contribution to the difference between melting and crystallization temperatures arising from both the temperature dependence of the fold surface free energy and the thickness increment above the minimum (thermodynamic) lamellar thickness. Neglecting these two factors causes an underestimation of the equilibrium melting temperature and overestimation of the thickening coefficient. Despite criticism, the Hoffman–Weeks procedure is still in use because of its simplicity, needing only the experimental melting temperature of the crystallites formed at T_c .

Notwithstanding the above limitations, the experimental melting temperatures (T_m) of the polyesters under investigation crystallized at different T_c s were used to obtain information on the equilibrium melting temperature T_m^0 by means of the Hoffman–Weeks' relationship [30]:

$$T_m = T_m^0(1 - 1/\gamma) + T_c/\gamma \quad (1)$$

where γ is a factor which depends on the lamellar thickness. More precisely $\gamma = l/l^*$ where l and l^* are the thickness of the grown crystallite and of the critical crystalline nucleus, respectively [34]. Note that Eq. (1) correctly represents experimental data only when γ is constant and the slope of the curve in the plot of T_m versus T_c is approximately equal to 0.5 [34].

The peak temperature of the endotherms II and III as a function of T_c is plotted in Fig. 7 for PPS, PPG, PPA and PPAz.

Endotherm II is clearly related to the original main crystal population and its location reflects the higher perfection of the crystals grown at higher temperatures. Melting endotherm III is observed at a rather constant temperature characteristic of the material partially recrystallized into a more stable form on heating. As a matter of fact, with the increment of T_c , the originally grown crystals improve their degree of perfection up to a point at which no further recrystallization can occur during the DSC run, and endotherm III disappears. The deviation from linearity found at low T_c values is symptomatic of the fast reorganization process involving imperfect crystallites during the DSC heating. In Fig. 6 the linear extrapolation of experimental data up to the $T_m = T_c$ line is also drawn, and T_m^0 values of 61, 67, 56 and 70 °C were found for PPS, PPG, PPA and PPAz, respectively. As regards PPS sample, the result appears in excellent agreement with the datum reported by other authors [19]. Up to now, to our knowledge, no data for T_m^0 of PPG, PPA and PPAz have been reported in the literature. As it can be seen, the odd–even effect is confirmed.

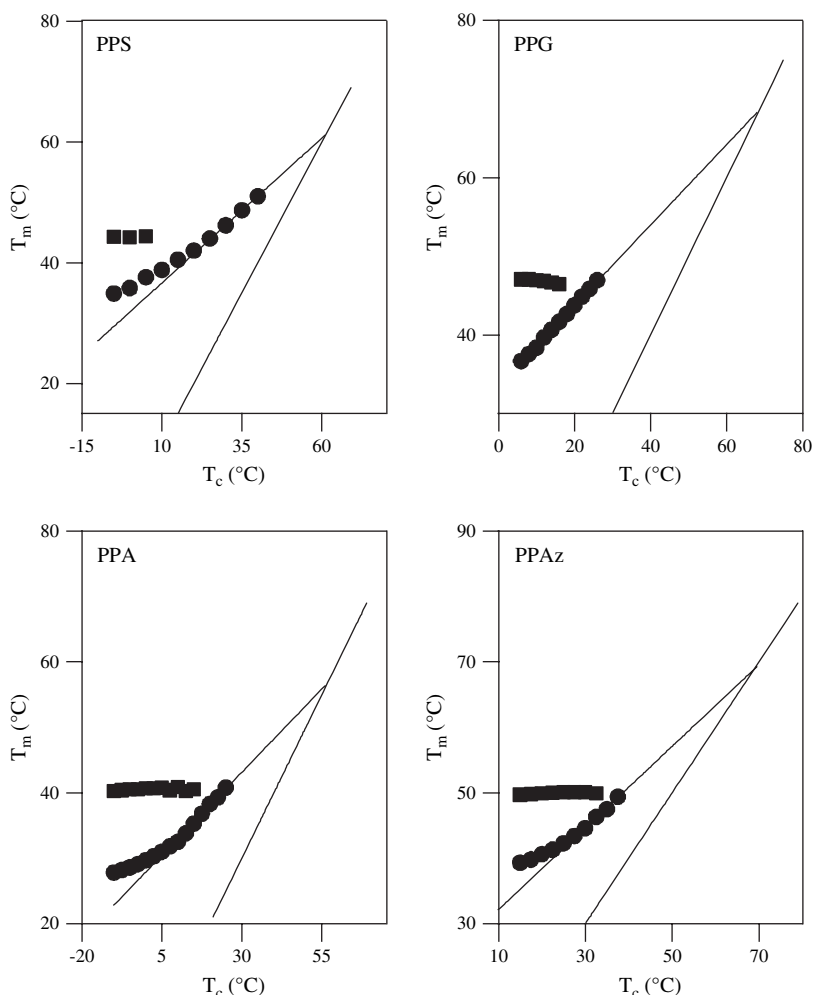


Fig. 7. Peak temperatures of (●) II and (■) III endotherms, scanned at 10 °C/min, as a function of T_c and linear extrapolation according to the Hoffman–Weeks treatment.

3.3.2. Crystallization kinetics

As well known, the analysis of the isothermal crystallization kinetics can be carried out on the basis of the Avrami equation [35]:

$$X_t = 1 - \exp[-k_n(t - t_{\text{start}})^n] \quad (2)$$

where X_t is the fraction of polymer crystallized at time t , k_n the overall kinetic constant, t is the time of the isothermal step measured from the achievement of the temperature control, t_{start} the initial time of the crystallization process, as described in Section 2, and n the Avrami exponent, which is correlated with the nucleation mechanism and the morphology of the growing crystallites. X_t can be calculated as the ratio between the area of the exothermic peak at time t and the total measured area of crystallization peak. The value of the kinetic constant k_n is also frequently obtained by means of the following relationship:

$$k_n = \ln 2/t_{1/2}^n \quad (3)$$

where $t_{1/2}$ is the crystallization half-time, defined as the time required to reach $X_t = 0.5$.

It is likewise worth remembering that Eq. (2) is usually applied to the experimental data in the linearized form, by plotting $[\ln(-\ln(1-X_t))]$ as a function of $\ln(t-t_{\text{start}})$, permitting the determination of n and k_n from the slope and the intercept, respectively. In Fig. 8, typical linearized Avrami plots for PPA and PPAz are shown for a selected set of crystallization temperatures.

As it can be noted, no data are reported for PPS and PPG. The isothermal crystallization kinetics of these two polyesters could not be investigated because of the too low crystallization rate. As far as PPS polyester is concerned, the result is in contrast with that reported by Bikiaris and Papageorgiou [19]. In their paper, the authors investigated the crystallization behaviour of a PPS sample, which, however, was characterized by a significantly lower molecular weight ($M_n = 6900$). Thus, the discrepancy is not surprising taking into account that crystallization rate significantly decreases as the molecular weight is increased.

The crystallization half-time $t_{1/2}$, the parameter n , and the kinetic constant k_n are collected in Table 2: as can be seen, for all the samples under investigation, the overall kinetic constant k_n regularly decreases with increasing T_c , as usual at low

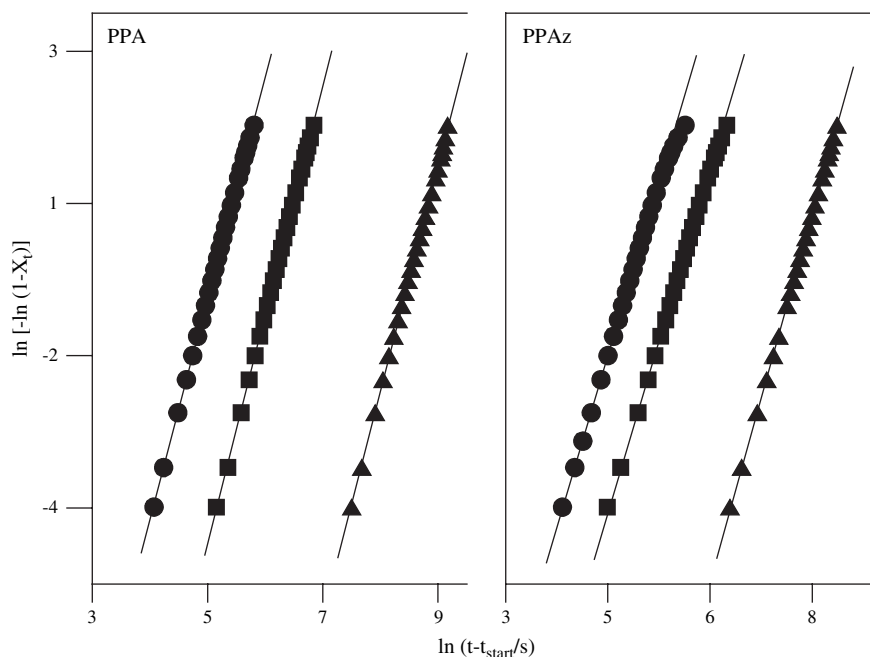


Fig. 8. Avrami plots at different T_c s for PPA: (●) 5 °C, (■) 12.5 °C, (▲) 25 °C; PPAz: (●) 27.5 °C, (■) 30 °C, (▲) 35 °C.

undercooling, where the crystal formation is controlled by nucleation.

In order to evaluate the effect of chemical structure on crystallization rate, the half-crystallization time $t_{1/2}$ was plotted as a function of undercooling degree ($\Delta T = T_m^0 - T_c$) in Fig. 9: it is evident that crystallization half-times of PPAz are lower than those of PPA.

It is worth remembering that the crystallite formation is controlled by several factors: first of all, it has to be reminded the thermodynamic requirements, which are correlated to the symmetry of the chains, which allows the regular close

packing, and to the presence of groups which encourage strong intermolecular attraction thereby stabilizing the alignment; in addition to the thermodynamic requirements, kinetic factors relating to the flexibility and mobility of the chain in the melt must also be considered. The enhanced crystallization rate of PPAz compared to the one of PPA, can be explained on the basis of an increment of chain flexibility.

As far as the Avrami exponent n is concerned, both for PPA and PPAz isothermally crystallized samples, it turned out to be close to 3 for all the crystallization temperatures investigated (see Table 2), indicating that the crystallization process

Table 2
Kinetic parameters for the isothermally crystallized PPA and PPAz polymers

Polymer	T_c (°C)	$t_{1/2}$ (min)	n	k_n (s ⁻ⁿ)
PPA	-5.0	2.5	2.9	1.2×10^{-05}
	-2.5	2.6	2.8	7.0×10^{-06}
	0.0	2.7	2.7	4.8×10^{-06}
	2.5	2.9	2.9	2.1×10^{-06}
	5.0	3.2	2.9	8.9×10^{-07}
	7.5	3.8	3.0	3.3×10^{-07}
	10.0	4.6	3.0	1.2×10^{-07}
	12.5	6.5	3.0	2.5×10^{-08}
	15.0	8.8	3.0	1.1×10^{-08}
	17.5	14.6	3.0	1.9×10^{-09}
	20.0	21.4	3.0	5.3×10^{-10}
PPAz	22.5	41.1	2.8	1.6×10^{-10}
	25.0	63.5	3.0	3.6×10^{-11}
	20.0	1.8	2.5	1.1×10^{-04}
	22.5	1.9	2.8	2.4×10^{-05}
	25.0	2.4	2.8	4.3×10^{-06}
	27.5	3.4	3.0	2.6×10^{-07}
	30.0	5.7	3.0	3.8×10^{-08}
	32.5	11.7	3.0	1.9×10^{-09}
	35.0	28.1	3.1	5.4×10^{-11}

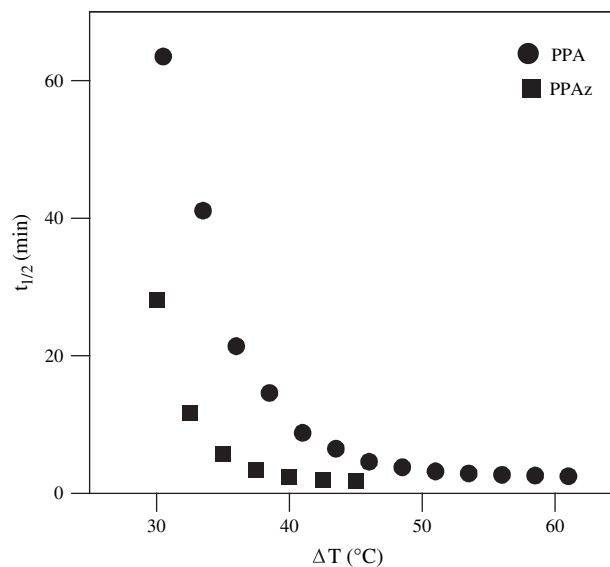


Fig. 9. Crystallization half-time as a function of undercooling degree for PPA and PPAz.

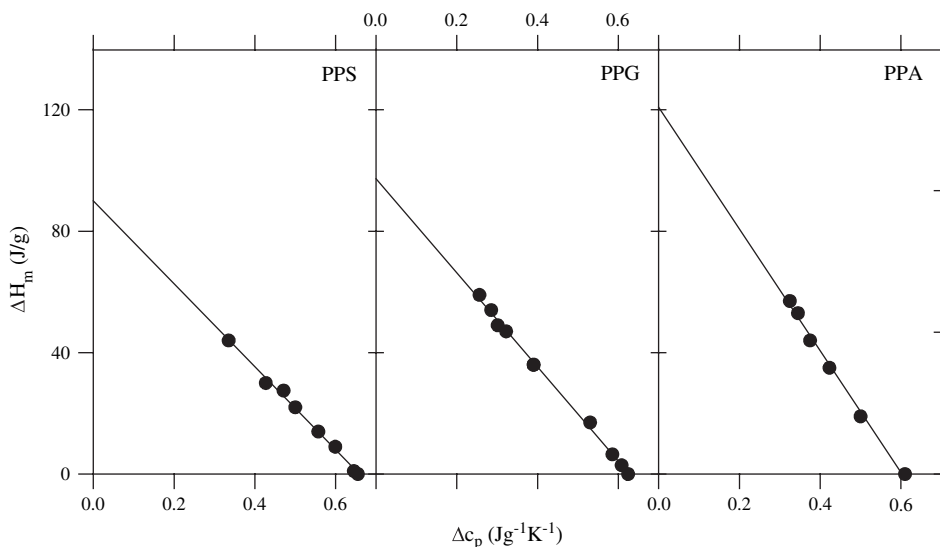


Fig. 10. ΔH_m as a function of Δc_p at T_g .

originates from predetermined nuclei and is characterized by three-dimensional spherulitic growth.

3.4. Rigid-amorphous phase

To evaluate the existence of a rigid-amorphous phase in the polyesters under investigation, we examined the relationship between Δc_p at T_g and ΔH_m of samples with different crystal/amorphous ratio. The ΔH_m values obtained were plotted as a function of the corresponding Δc_p in Fig. 10: in all cases, the specific heat increment is seen to decrease regularly as the melting enthalpy increases and a very good linear fit is obtained.

The extrapolation to $\Delta c_p = 0$ of the best fit of the $\Delta H_m - \Delta c_p$ data gives values of 91, 97 and 120 J/g for PPS, PPG and PPA, respectively, in good agreement with those (95, 102 and 124 J/g, respectively) calculated with the van Krevelen approach based on group contributions [36]. The agreement between the value extrapolated by the experimental data and the one calculated with the van Krevelen approach is a clear evidence that for PPS, PPG and PPA interphase formation has not to be hypothesized in contrast with the results obtained previously on poly(butylene terephthalate), poly(propylene terephthalate) and poly(ethylene terephthalate) [14,15,37]. No investigation was carried out on PPAz polyester because samples with different amorphous/crystal ratio cannot be obtained, due to its too high crystallization rate.

4. Conclusions

The results obtained showed the possibility of easily synthesizing in bulk, by the usual two-stage polycondensation procedure, novel aliphatic polyesters based on 1,3-propanediol and characterized by different chain length of dicarboxylic acid subunit having molecular weights higher than those of polymers belonging to the same class.

The data concerning the thermal characterization display that the number of carbon atoms in the repeat unit lead to

significant variations in the final properties of PPS, PPG, PPA and PPAz. In particular:

- the thermal stability of the polyesters follows a complex trend, which can be explained on the basis of several factors, among these the increment of the number of $-\text{CH}_2-$ in the polymeric chain;
- the glass transition temperature decreases as the number of methylene groups in the repeat unit is increased, due to an increment of macromolecular chain flexibility;
- the melting point shows an odd–even fluctuation, due to several factors, like chain flexibility, chain conformations and crystal structure;
- the ability to crystallize increases as the number of methylene groups is increased, due to an increment of macromolecular chain flexibility.

In conclusions, the results here reported confirm that the chemical structure is a very important factor in controlling the final properties of a polymeric material.

References

- [1] Gross RA, Kalra B. *Science* 2002;297:803–10.
- [2] Amass W, Amass A, Tighe B. *Polym Int* 1998;47(2):89–144.
- [3] Braunneg G, Lefebvre G, Genser KF. *J Biotechnol* 1998;65(2–3):127–61.
- [4] Doi Y. *Microbial polyesters*. New York: VCH Publishers Inc.; 1990.
- [5] Okada M. *Prog Polym Sci* 2002;27(1):87–90.
- [6] Yamamoto M, Witt U, Skupin G, Beimborn D, Müller RJ. In: Doi Y, Steinbüchel A, editors. *Biopolymers*, vol. 4. Weinheim, Germany: Wiley-VCH; 2002. p. 299–314 [chapter 3].
- [7] Müller RJ, Kleeberg I, Deckwer WD. *J Biotechnol* 2001;86(2):87–95.
- [8] Schauhoff S. *Chem Fiber Int* 1996;46(4):263–4.
- [9] Kelsey DR. U.S. Patent 6,200,093,786, 2000.
- [10] Wang B, Li CY, Hanzlicek J, Cheng SZD, Geil PH, Grebowicz J, et al. *Polymer* 2001;42(16):7171–80.
- [11] <http://www.dupont.com/sonora:apps.html>.
- [12] <http://www.shell.com>.
- [13] Schick C, Wigger J, Mischoc W. *Acta Polym* 1990;41:137.

- [14] Cheng SZD, Wu ZQ, Wunderlich B. *Makromol Chem* 1988;189:2443.
- [15] Sisti L, Finelli L, Lotti N, Berti C, Munari A. *e-Polymers* 2003. no. 054.
- [16] Toshihiko J, Shigeo A, Masao S. *J Macromol Sci Phys B* 1997;36:381.
- [17] Huo P, Cebe P. *Macromolecules* 1992;25:902.
- [18] Righetti MC, Munari A. *Macromol Chem Phys* 1997;198(2):363–78.
- [19] Papageorgiou GZ, Bikiaris DN. *Polymer* 2005;46:12081–92.
- [20] Goodman I. *Encyclopedia of polymer science and engineering*. 2nd ed., vol. 12. New York: Wiley; 1988. p. 1–75.
- [21] Plage B, Schulten HR. *Macromolecules* 1990;23(10):2642–8.
- [22] Korshak VV, Vinogradova SV. *Polyesters*. Oxford: Pergamon Press; 1965 [chapter 6].
- [23] Boyer RF. *Rubber Chem Technol* 1963;36:1303.
- [24] Fuller CS, Frosch CJ, Pape NR. *J Am Chem Soc* 1942;64:154–60.
- [25] Blundell J, Osborn BN. *Polymer* 1983;24(8):953–8.
- [26] Lee Y, Porter RS. *Macromolecules* 1989;22(4):1756–60.
- [27] Rim PB, Runt JP. *Macromolecules* 1984;17(8):1520–6.
- [28] Marand H, Alizadeh A, Farmer R, Desai R, Velikov V. *Macromolecules* 2000;33(9):3392–403.
- [29] Chung JS, Cebe P. *Polymer* 1992;33(11):2325–33.
- [30] Hoffman JD, Weeks JJ. *J Res Nat Bur Stand* 1962;66A(1):13–28.
- [31] Xu J, Srivatsan S, Marand H, Agarwal P. *Macromolecules* 1998;31(23):8230–42.
- [32] Marand H, Xu J, Srinivas S. *Macromolecules* 1998;31(23):8219–29.
- [33] Al-Hussein M, Strobl G. *Macromolecules* 2002;35(5):1672–6.
- [34] Lee SW, Lee B, Ree M. *Macromol Chem Phys* 2000;201(4):453–63.
- [35] Avrami M. *J Chem Phys* 1941;9:177–84.
- [36] Van Krevelen DW. *Properties of polymers*. New York: Elsevier; 1990.
- [37] Vannini M, Finelli L, Lotti N, Colonna M, Lorenzetti C, Munari A. *J Polym Sci Part B Polym Phys* 2005;43:1441–54.